J Appl Biotechnol Rep. 2024 December;11(4):1479-1487

Journal of
Applied Biotechnology Reports

doi 10.30491/jabr.2024.423799.1686

Original Article

Production and Evaluation of Uniform Magnetic T-2 Imprinted Polymer from Aqueous Medium

Seyed Javad Davarpanah [1], **Ramin Karimian** [2*]

[1] Applied Biotechnology Research Center, Baqiyatallah University of Medical Science, Tehran, Iran
[2] Chemical Injuries Research Center, Systems Biology and Poisonings Institute, Baqiyatallah University of Medical Sciences, Tehran, Iran

Corresponding Author: Ramin Karimian, PhD, Associate Professor, Chemical Injuries Research Center, Systems Biology and Poisonings Institute, Baqiyatallah University of Medical Sciences, Tehran, Iran. Tel: +98-2182484522, E-mail: karimian.r@gmail.com

Received November 4, 2023; **Accepted** February 28, 2024; **Online Published** December 30, 2024

Abstract

Introduction: Mycotoxins are harmful secondary metabolites produced by fungi on agricultural products under various climatic conditions. In this study, we developed a method for the extraction and preconcentration of T-2 toxin from aqueous media using magnetic molecular imprinting polymers. This technique involves creating polymers with high recognition properties for specific molecules and has been widely utilized in diverse scientific and technical applications. The objective of the study was to assess the binding properties of the magnetic MIPs for T-2 extraction and determine their potential as an efficient sample preparation technique.

Materials and Methods: Magnetic T-2 imprinted nanoparticles using T-2 toxin (T-2) as the template, along with Methacrylic acid and ethyleneglycoldimethacrylate as the functional monomer and cross-linker were synthesized in aqueous media and characterized. We investigated their selective adsorption ability, adsorption kinetics, and isotherms. The selective extraction of T-2 toxin from aqueous media was performed.

Results: Our findings showed that under ambient conditions, the magnetic molecularly imprinted polymer nanoparticles (MMIP NPs) successfully extracted 70% to 81% of the T-2 toxin from the aqueous media after three times of recycling.

Conclusions: This study developed a method to create uniform magnetic T-2 imprinted nanoparticles. The technique holds promise for detecting and analyzing T-2 contamination in food and feed products. Magnetic molecularly imprinted nanoparticles have several advantages, including selective recognition, stability, reusability, and enhanced sensitivity.

Keywords: Uniform Magnetic Molecularly Imprinted Nanoparticle, T-2 Toxin, Relative Standard Seviation, Adsorption Kinetic, Adsorption Isotherm

Citation: Davarpanah SJ, Karimian R. Production and Evaluation of Uniform Magnetic T-2 Imprinted Polymer from Aqueous Medium. J Appl Biotechnol Rep. 2024;11(4):1479-1487. doi:10.30491/jabr.2024.423799.1686

Introduction

Mycotoxins refer to harmful secondary metabolites produced by fungi under various climatic conditions on agricultural products. These mycotoxins can have toxic effects, including carcinogenic, neurotoxic, nephrotoxic, immunosuppressive, and estrogenic properties. The presence of these secondary metabolites in food, beverages, and animal feed poses significant risks to human and animal health. It is important to note that mycotoxins exhibit a wide range of structural and chemical diversity, with approximately 400 known metabolites possessing toxic potential. These mycotoxins are produced by approximately 100 different molds, as documented in the scientific literature.[1-3]

Fusarium molds are a source of mycotoxins called trichothecenes (TCTC), which are found in cereals such as corn, oats, wheat and barley.[4,5] These toxins can damage cells, suppress the immune system, and inhibits the synthesis of DNA and RNA.[6,7] TCTC can be classified into four groups: A, B, C and D. The most relevant groups are A and B, which differ by the type of functional group at the C-8 position, ketone for type A and carbonyl for type B. The main representatives of type B TCTC are deoxynivalenol (DON) and nivalenol (NIV), while the major type A TCTC are T-2 toxin (T-2) and HT-2 toxin (HT-2) (Figure 1). DON is the most common TCTC, but T-2 is much more toxic, up to ten times more.[7,8] T-2 and HT-2 have been detected in *Fusarium sporotrichioides*, *Fusarium poae*, *Fusarium equiseti*, *Fusarium langsethiae* and *Fusarium acuminatum*.[1,9] The SCOOP Task 3.2.10 suggested that more data on T-2 and HT-2 levels in European cereals are needed and that more sensitive methods should be developed.[10]

Selective and sensitive methods are needed to analyze T-2 in complex food matrices. Some of the methods that have been used include thin-layer chromatography (TLC), gas chromatography-mass spectrometry (GC-MS), high-performance liquid chromatography (HPLC) with fluorescence detection (FLD), high-performance liquid chromatography-mass spectrometry (HPLC-MS), and LC-MS/MS.[4,7,11,12] To extract TCTC from food matrices, acetonitrile/water or methanol/water mixtures have been commonly used.[4,11-13] Before analysis, the extract has to be purified to eliminate matrix impurities and concentrate the analyte. Different clean-up techniques have been reported, such as IAC,[14] SPE

using MycoSep® columns,[4,15] OASIS HLB® columns,[4] charcoal/alumina cartridges[11] or a combination of florisil and cation exchange sorbents.[16] However, except for IAC, these techniques rely on non-specific interactions to retain the TCTC, which may result in impurities in the eluate after clean-up. IAC has some drawbacks as well, such as its instability in organic, acid or basic media, limited reuse and the time-consuming, costly production and isolation of antibodies.

Molecular imprinting is a technique that creates polymers with high recognition properties for specific molecules.[17-20] These polymers, called molecular imprinted polymers (MIPs), have recognition sites that match the size and shape of the target molecule (template) and have functional groups that interact with it. The process of molecular imprinting involves polymerizing functional and cross-linking monomers in the presence of the template. The template binds to the functional monomers and forms a pre-polymerization complex. Then, the polymerization is initiated by 2,2'-azobisisobutyronitrile, ultraviolet light or heat, and a cross-linking monomer fixes the functional monomers around the template in a dense polymer network. After the polymerization, the template is removed from the imprinted polymer, leaving behind binding sites that are complementary to the template in size and shape. These binding sites resemble the binding sites of antibodies and enzymes.[21-23] MIPs have been used as materials for molecular recognition and purification in various scientific and technical fields, such as solid phase extraction, chromatographic separation, membrane separations, sensors (Nanobiosensors and Optical biosensors), medical diagnostics, drug release, catalysts and so on.[24-28] Recently, new types of MIPs, such as nano magnetic MIPs have been developed. They have potential applications in biological and environmental fields because they combine the magnetic properties of nanoparticles with the high selectivity of MIPs for the target molecule. This allows the target molecule to be separated from different samples by using a magnetic field.[29] This study was based on previous reports that used MIPs for the determination and extraction of T-2 from water and fruit.[17,30-33] The purpose of this study was to develop and optimize magnetic nanoparticles that are imprinted with T-2, a pesticide, and to evaluate their binding properties for sample preparation and preconcentration of T-2 from aqueous media. We used HPLC-UV as a method to determine the amount of T-2 in aqueous media, because it is fast, easy, affordable and accessible. The magnetic MIPs were prepared using T-2 toxin as the template molecule and were used for directly extracting from water-based solutions. The extraction and clean-up processes were combined into a single step, simplifying the sample preparation procedure. This resulted in a significant reduction in both extraction time and the amount of solvent used. Unlike other methods that require manually grinding and blending the sample with a sorbent, this step was eliminated and replaced with magnetic stirring. This change not only simplified the subsequent treatment by allowing easy separation of the nano magnetic MIPs from the sample matrix but also greatly reduced the coextracts. Additionally, the polymer material could be reused.

Materials and Methods

Chemicals and Materials

Iron chloride, Ferric chloride, Ammonium hydroxide (25%), Methacrylic acid (MAA), T-2 toxin, Deoxynivalenol (DON), Tetraethoxysilane (TEOS), 3-methacryloyloxypropyltrimethoxysilane (MPS), and Ethyleneglycoldimethacrylate (EGDMA) were obtained from Sigma–Aldrich (Milwaukee, USA). 2,2'-azobisisobutyronitrile (AIBN), Igepal Co-520 and Tween 80 were purchased from Acros (Geel, Belgium).

Synthesis of Fe_3O_4@MIPs and Fe_3O_4@NIPs

Fe_3O_4 nanoparticles (NPs) were synthesized using a previously reported method. In brief, a mixture of 0.60 g $FeCl_2 \cdot 4H_2O$, 1.57 g $FeCl_3 \cdot 6H_2O$, and 2 ml highly purified water, along with 4% Tween 80, was added to 60 ml purified soybean oil under mechanical stirring at 3000 rpm until a nearly clear emulsion was obtained. This solution was referred to as solution A. Subsequently, a solution of 0.35 g NaOH dissolved in 2.5 ml water was added drop by drop to solution A under mechanical stirring at 2000 rpm for 2.5 hours at room temperature. The resulting reaction mixture was then filtered, and the precipitate was washed three times with 500 ml absolute water to remove any unreacted chemicals. The material was further calcinated at 220 °C for 3 hours in an electric oven. To prepare the magnetic NPs, 30 mg of the Fe_3O_4 NPs were dissolved in a mixture of 11 ml cyclohexane and 2 ml Igepal Co-520 by sonication for 10 minutes. Then, 2 ml of ammonium hydroxide and 2.5 ml of TEOS were sequentially added to the mixture. The reaction was carried out under continuous mechanical stirring at room temperature for 12 hours. The resulting product was collected using an external magnetic field, rinsed thoroughly with highly purified ethanol three times, and dried under vacuum. Next, 20 mg of Fe_3O_4@SiO_2 was dissolved in 30 ml methanol by sonication for 10 minutes. Then, 0.5 ml of MPS was added drop by drop to the solution, and the mixture was reacted under continuous stirring at room temperature for 48 hours. The resulting product was collected using an external magnetic field, rinsed thoroughly with methanol, and dried under vacuum.[30] To imprint the template, a solution containing 0.2 mM of T-2 (as the template) and 0.4 mM of MAA (as the functional monomer) dissolved in 5 ml chloroform was shaken in a water bath at 25 °C for 12 hours. Then, 20 mg of Fe_3O_4@SiO_2@MPS MNPs was added to the solution and shaken for 2 hours. Subsequently, 0.2 mM of EGDMA and 0.5 mM of AIBN were added to the system, and the mixture was sonicated in a water bath for 1 minute. After purging the system with nitrogen gas for 5 minutes to

remove oxygen, the reaction was carried out at 60 °C under nitrogen gas for 12 hours to complete the polymerization process. To remove the template, the polymers were washed sequentially with pure water, methanol-acetic acid (7:3, v/v), and acetonitrile until no T-2 absorption was detected using an HPLC spectrophotometer. The resulting product, uniform magnetic molecularly imprinted nanoparticles (MMINPs), was dried at 30 °C under vacuum. For comparison purposes, magnetic non-molecular imprinted polymers (NMMNIPs) were prepared under the same conditions as described above, but without the addition of the T-2 template.[30]

Binding Experiments of Fe_3O_4@MIPs and Fe_3O_4@NIPs

In the kinetic adsorption experiments, the procedure involved regenerating of 60 mg of sorbent (MIP or NIP) using 10 ml of methanol-acetic acid solution (7:3, v/v), followed by 10 ml of acetonitrile (ACN) and 5 ml of deionized water. Subsequently, Fe_3O_4@MIPs or Fe_3O_4@NIPs were added to 10 ml of a T-2 solution with a concentration of 10 mg/L. The mixture was then incubated for specific time intervals ranging from 1.5 to 45 minutes. Afterward, the supernatant and polymers were separated using an external magnetic field. The concentration of T-2 in the supernatants was determined through HPLC-UV analysis. The HPLC method was also employed to determine the amount of T-2 bound to the Fe_3O_4@MIPs or Fe_3O_4@NIPs.

In the isothermal binding experiments, the process involved regenerating the polymer (MIP or NIP), followed by the addition of 60 mg of either Fe_3O_4@MIPs or Fe_3O_4@NIPs to a 10 ml acetonitrile solution containing varying concentrations of T-2, ranging from 0.50 to 20 mg/L. The mixture was then incubated at room temperature for 15 minutes. Subsequently, the supernatants and polymers were separated using an external magnetic field, and the concentration of T-2 in the supernatants was determined through HPLC-UV analysis.

Selective Recognition of Fe_3O_4@MIPs and Fe_3O_4@NIPs

10 mg of Fe_3O_4@MIPs or Fe_3O_4@NIPs were added to a 10 ml acetonitrile solution containing a mixture of T-2 (10 mg/L) and DON (10 mg/L). The mixture was incubated for 30 minutes at room temperature. Subsequently, the supernatants and polymers were separated using an external magnetic field, and the amounts of T-2 and DON in the supernatants were measured using HPLC-UV.

Extraction of T-2 from Aqueous Samples

First, 60 mg of Fe_3O_4@MIPs were regenerated with 10 ml of methanol-acetic acid (7:3, v/v) and 10 ml of ACN, and conditioned with 5 ml of deionized water added to 5 ml of T-2 (10 ppm). The mixed sample was shaken for 30 minutes and sonicated for 10 minutes to extract T-2. The supernatants and polymers were separated by an external magnetic field. Finally, after discarding the supernatant solution, the Fe_3O_4@MIPs that had absorbed the target molecule were eluted with methanol-acetic acid (7:3, v/v), and the elution was collected, evaporated to dryness under a stream of nitrogen. The residue was then dissolved in 5 mL of methanol-water (3:7, v/v). The concentration of T-2 was determined by HPLC-UV.

Results and Discussion

Synthesis of Magnetic T-2 Imprinted Nanoparticles

Figure 1. illustrates the principle for the preparation of Fe_3O_4@SiO_2@MIP particles. Initially, magnetic Fe_3O_4 nanoparticles were synthesized using the inverse microemulsion method. Subsequently, the Fe_3O_4 particles were coated with SiO_2 through the sol-gel process, resulting in Fe_3O_4@SiO_2 particles. The silica coating provides several advantages to the magnetic nanoparticles, including improved dispersion in liquid media, protection against leaching, and a surface that can be easily modified with various groups for MIP preparation. Next, the surface of Fe_3O_4@SiO_2 particles was modified with polymerizable vinyl end groups, leading to the formation of vinyl-modified Fe_3O_4@SiO_2 particles through the sol-gel process. This modification ensured a tighter grafting of the molecularly imprinted polymer (MIP) on the surface of the Fe_3O_4@SiO_2 particles.[30] Subsequently, in the presence of the T-2 template, functional monomer (MAA), cross-linker agent (EGDMA), and the vinyl-modified Fe_3O_4@SiO_2 particles, polymerization took place at the surface of the vinyl-modified Fe_3O_4@SiO_2 particles. The resulting Fe_3O_4@SiO_2@MIP particles were collected using an external magnetic field. Additionally, Fe_3O_4@SiO_2@NIP nanoparticles were prepared under the same conditions but without the T-2 template.

Characterization of Magnetic T-2 Imprinted Nanoparticle

Morphology and size of MMIP nanoparticles were measured using an SEM instrument. FT-IR spectra were recorded in the range of 4000–400 cm^{-1}. The identification of the crystalline phase of MMIPs was performed using an X-ray diffractometer over the 2θ range of 10–80°.[30]

As can be observed the morphology of T-2 imprinted polymer was evaluated by SEM from the resulting patterns in Figure 2. It is obviously seen that the magnetite microspheres were uniformly dispersed. The size of the MIP NPs was about 30-70 nm. So, the imprinting layer has a uniform thickness and a relatively narrow size distribution. The MIP NPs have a large and specific surface area that enables them to selectively adsorb the target molecule.

Fe_3O_4@MIPs were investigated by FT-IR spectroscopy (Figure 3). The characteristic peaks of Fe-O at 572 cm^{-1}, Si-O-Si group at about 1101 cm^{-1} and OH group at about 1649 and 3439 cm^{-1} indicate the formation of silica coating on the surface of Fe_3O_4.

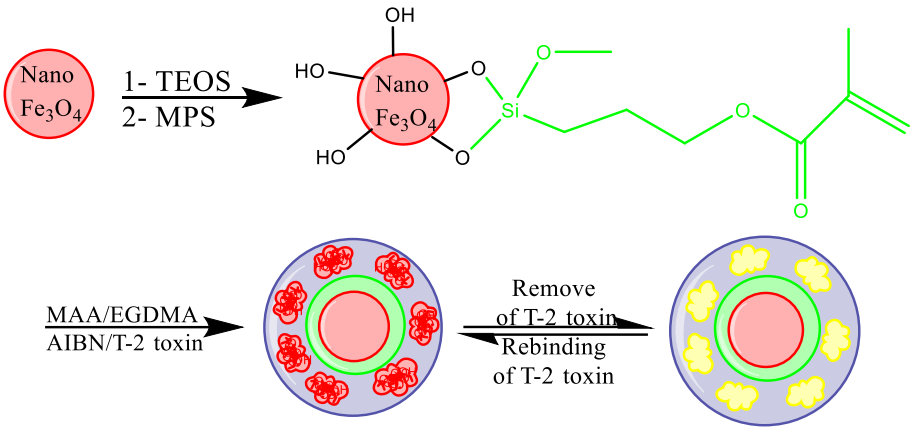

Figure 1. Scheme of Preparation of Fe_3O_4@SiO_2@MIP.

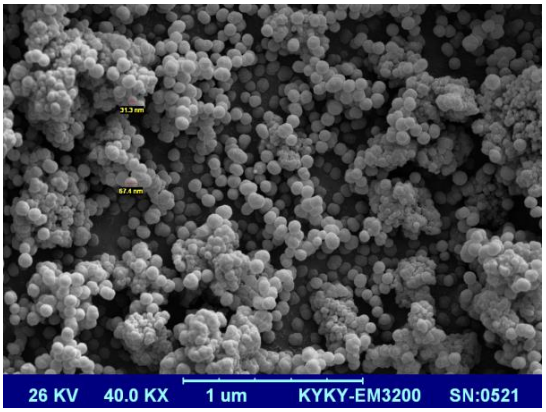

Figure 2. SEM of Fe_3O_4@MIP NPs.

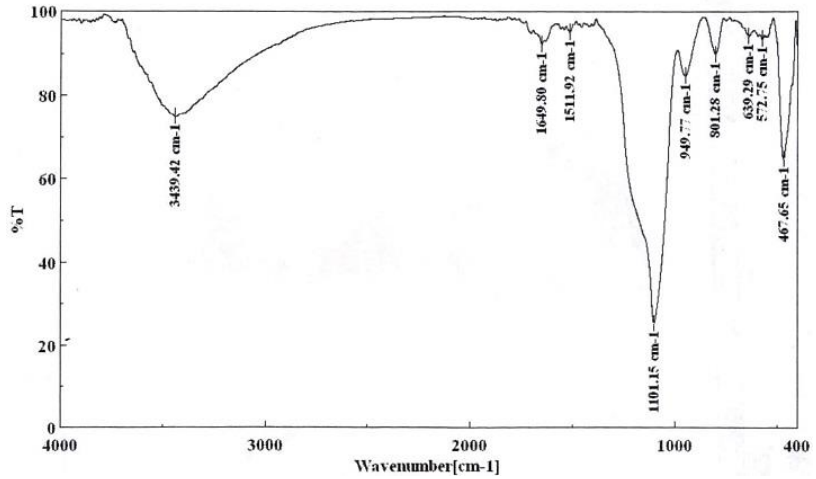

Figure 3. FT-IR Spectra of Fe_3O_4@MIPs.

XRD analysis was used to examine the structural properties of the magnetic T-2 imprinted nanoparticles. Figure 4 shows the XRD pattern of the magnetic T-2 imprinted nanoparticles, which exhibit several relatively strong diffraction peaks in the 2θ range of 10–80°. These peaks indicate that the synthesized magnetic absorbent nanoparticles are highly crystalline materials. The six discernible diffraction peaks (30.4°, 35.5°, 43.26°, 53.63°, 57.2°, and 62.79°) in Fig. 4 match well with the database of magnetite in the JCPDS (JCPDS Card: 19-629) file.

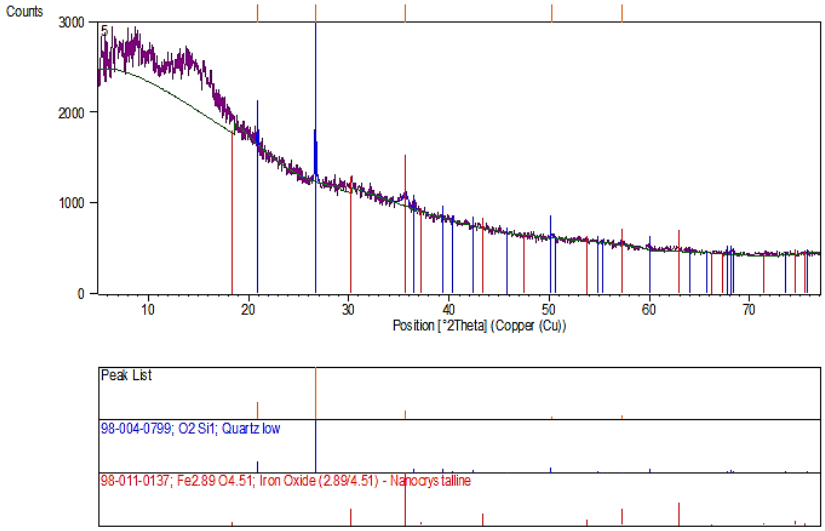

Figure 4. XRD Pattern of Fe_3O_4@MIP.

Binding Experiments of Fe_3O_4@MIPs and Fe_3O_4@NIPs

During the kinetic adsorption experiments, 60 mg of sorbent (MIP or NIP) was initially regenerated using 10 ml of methanol-acetic acid (7:3, v/v), followed by 10 ml of ACN and 5 ml of deionized water. Subsequently, Fe_3O_4@MIPs or Fe_3O_4@NIPs were introduced into a 10 ml solution containing 10 mg/L of T-2, and the mixture was incubated for various time intervals ranging from 1.5 to 45 minutes. After separating the supernatant and polymers using an external magnetic field, the concentration of T-2 in the supernatant was determined through HPLC-UV analysis. The amount of T-2 bound to the Fe_3O_4@MIPs or Fe_3O_4@NIPs was determined using an HPLC method.

In the isothermal binding experiment, 60 mg of regenerated polymer (MIP or NIP) was added to a 10 ml acetonitrile solution containing different concentrations of T-2, ranging from 0.50 to 20 mg/L, and incubated for 15 minutes at room temperature. The supernatants and polymers were separated using an external magnetic field, and the concentration of T-2 in the supernatant was measured using HPLC-UV.

The recognition ability of T-2 with Fe_3O_4@MIPs NPs was investigated through an adsorption kinetics test. The adsorption kinetics of a 10 mg/L T-2 solution onto Fe_3O_4 @MIPs and Fe_3O_4@NIPs is shown in Figure 6A. The adsorption process consisted of two steps: a fast step and a slow step. In the first step, the adsorption rate was high, and it took approximately 180 seconds to reach near equilibrium. In the second step, the adsorption rate was low until equilibrium was achieved. It can be observed that the adsorption capacity increased over time, and the imprinted NPs exhibited a rapid adsorption rate. The adsorption capacity increased rapidly within the first 15 seconds and almost reached equilibrium after 180 seconds. In this study, the equilibrium time of Fe_3O_4@MIPs was shorter compared to other surface imprinting technologies for T-2. The imprinted Fe_3O_4@MIPs only required 15-180 seconds to reach adsorption equilibrium for the template molecules, indicating that they possessed good mass transport properties and overcame some limitations of traditional packed imprinted materials.

Equilibrium experiments were conducted to evaluate the binding affinity of T-2 to the imprinted particles. The binding isotherm of T-2 with the MIP and NIP was determined within the concentration range of 2 to 50 mg/L, in the presence of 60 mg of MMIP or MNIP, at room temperature. The results revealed that the quantity of T-2 bound to the magnetic imprinted polymer was greater compared to that bound to the magnetic non-imprinted polymer, indicating that the imprinted binding sites contribute to a higher affinity binding. Consequently, the maximum binding capacity of MMIPs for T-2 was significantly higher than that of MNIPs. The Scatchard equation is a useful tool for evaluating the adsorption parameters and the types of binding sites in the MIP. The equation is given by:

$$\frac{Q}{C_{t-2}} = \frac{Q_{max} - Q}{K_d}$$

In the equation, Q represents the amount of T-2 bound to the MMIPs or MNIPs at equilibrium, C_e denotes the concentration of free T-2 at equilibrium. K_d is the dissociation constant, and Q_{max} is the apparent maximum binding amount. The values of K_d and Q_{max} can be calculated from the slope and intercept of the linear line plotted in Q/C_e versus Q. The Scatchard plot was performed for Fe_3O_4@MIPs. According to the Scatchard plot, adsorption occurred uniformly on the active sites of the adsorbent. Once a template molecule

occupied a site, further adsorption could not take place at that site. The experimental data were observed to fit the Scatchard plot adsorption isotherm model (Figure 6C). The linear regression equation for the linear region is Q/[T-2] = 0.026 - 0.0562Q (r^2 = 0.9087). From the obtained slope and intercept of the straight line, the values of K_d (K_d = -1 / slope) and Q_{max} (Q_{max} = intercept) were calculated as 17.79 × 10^{-5} mol/L and 0.026 µM/g, respectively.

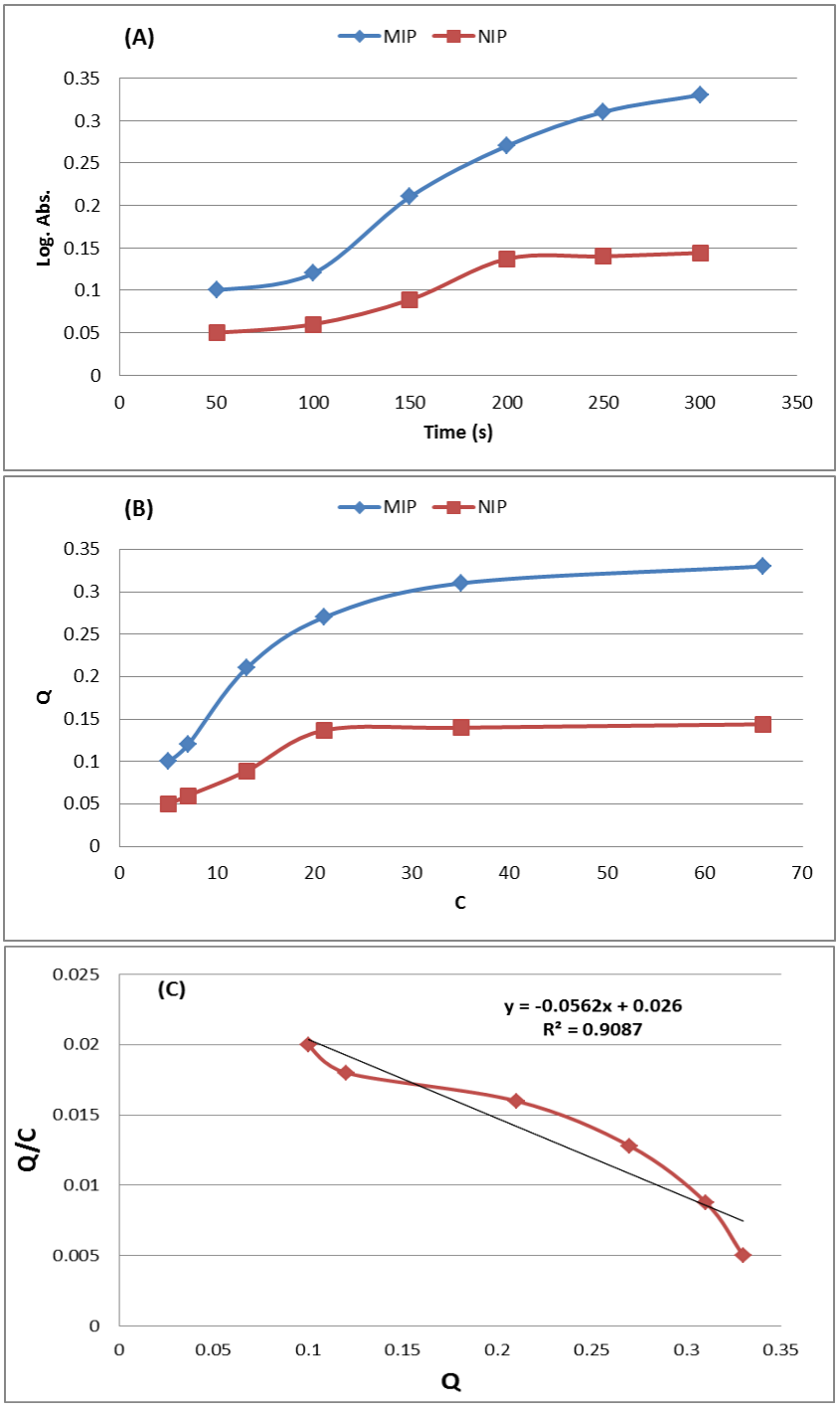

Figure 5. Adsorption kinetics of MIPs and NIP nanoparticles (A); Adsorption isotherm of T-2 onto MIPs and NIP nanoparticles (B); Scatchard analysis curves of Fe_3O_4@MIPs (C).

Selective Recognition of Fe_3O_4@MIPs

To study the selective recognition of T-2, DON, which has a similar size and structure to T-2, was used as a competitor. In these experiments, the distribution coefficient (K_d) and the selectivity coefficient (k) of the T-2 sorbent were calculated. The distribution coefficient shows the ratio of the amount of sorbent-bound analytes to the amount of free analytes in the supernatant. The selectivity coefficient shows

the difference in adsorption between the two substances, and it is defined as k = $K_{d(T-2)}/K_{d(DON)}$ (54.7/2.11 = 25/8 ≈ 26). On the NIP sorbent, T-2 and DON had similar K_d values. However, on the MIP sorbent, T-2 had more than twenty times higher adsorption capacity than DON.

Extraction of T-2 from Infected Aqueous Samples

The initial experiments (before T-2 spiking) showed that there was a small amount of T-2 in the infected aqueous media and we could not find a sample without toxin. Thus, the additional standard method was applied in the calibration procedure. It meant that T-2 was spiked into the aqueous medium which contained a fixed amount (X ppm) of this toxin. The standard curve was obtained from HPLC-UV analysis. Due to the low sensitivity of HPLC-UV, the minimum concentration determined in standard solutions was 2 ppm. Thus, the standard curve was also plotted in the range of 2–50 ppm. The standard calibration curve of the peak area versus the concentrations of T-2 is shown in Figure 7.

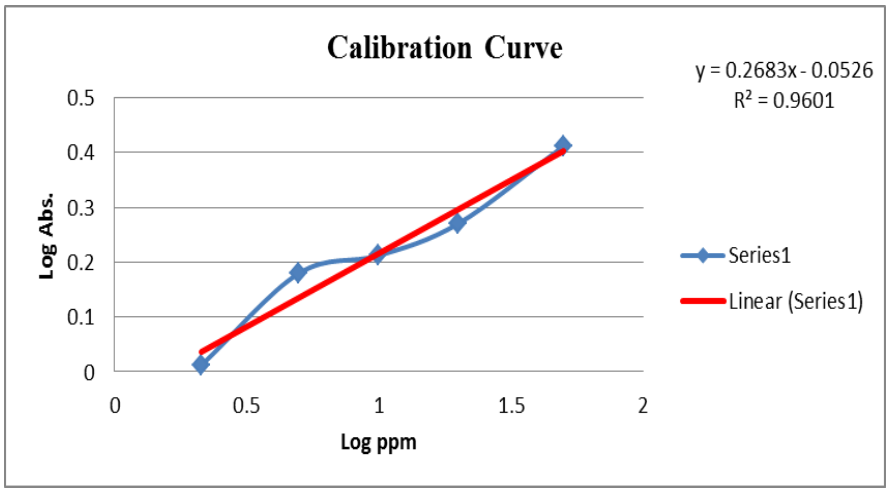

Figure 6. Linear Range of the Calibration Curve for the T-2 at the Optimized Condition.

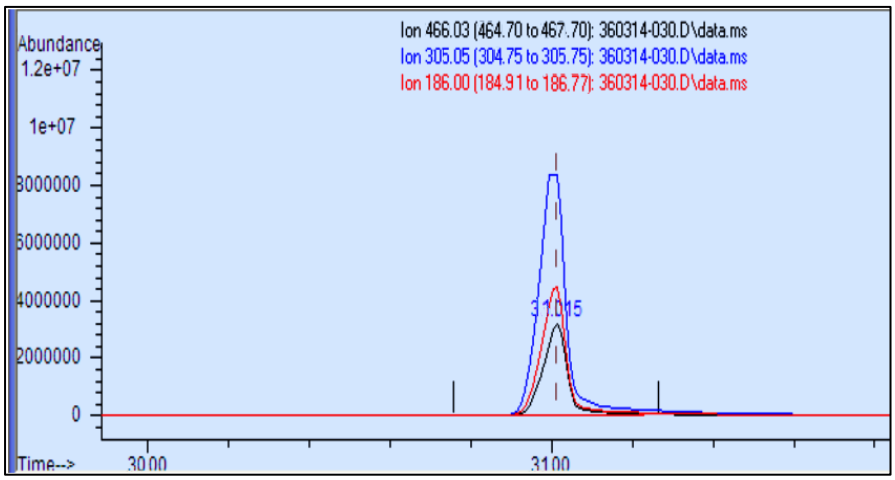

Figure 7. The GC-Mass Chromatograms of a Standard Solution of T-2an Aqueous Sample.

The calibration plot for T-2 was linear over the concentration range of 2 to 50 mg/l. The calibration linear equation was y = 0.2683×C_{T-2} - 0.0526, and a linear regression coefficient (R^2) of 0.9601 was obtained under optimal conditions. The limit of detection (LOD) was calculated based on the minimum distinguishable signals (S = 0.1448) and the slope (m = 0.2683) of the linear regression for lower concentrations of the template using the equation: LOD = 3S/m. The LOD of T-2 was determined to be 1.62 mg/l. The repeatability, based on the relative standard deviation (RSD%), was approximately 66.69%. The recovery extraction of T-2 from aqueous samples was found to be 70-81%. Figure 7 illustrates the chromatograms of a standard solution of T-2, an aqueous sample with the same concentration after the extraction of T-2 (three times), and GC-Mass analysis.

Conclusion

In this study, an efficient method was developed to prepare uniform magnetic molecularly imprinted nanoparticles using T-2 as a template. We synthesized magnetic Fe3O4 nanoparticles and modified their surfaces to disperse in organic solvents, enabling their participation in the molecularly imprinted polymerization process. The resulting Fe3O4@MIP and Fe3O4@NIP (non-imprinted polymer) nanoparticles underwent characterization using SEM, FT-IR, and XRD analyses. The developed method demonstrated its effectiveness in quantifying T-2 within a concentration range of 2-20 ppm in aqueous media samples, with achieved recoveries ranging from 70% to 81%. The study also investigated the adsorption behaviors of the nanoparticles using high-performance liquid chromatography with ultraviolet detection (HPLC-UV), encompassing their selective adsorption ability, adsorption kinetics, and isotherms. The technique show cased significant potential for the selective extraction and quantification of T-2, and it could be extended to other compounds as well. The utilization of these magnetic molecularly imprinted nanoparticles presents a promising approach for the detection and analysis of T-2 contamination in food and feed products. In summary, the study introduces a novel method for the production of uniform magnetic molecularly imprinted nanoparticles, enabling selective extraction and quantification of T-2. The results highlight the efficacy of the developed technique and its potential applicability in ensuring food and feed product safety with regards to T-2 contamination.

Overall, the advantages of MMIPs include their selective recognition, stability, reusability, and enhanced sensitivity. This allows for the separation of MMIPs using an external magnetic field. The magnetic responsiveness facilitates rapid and efficient sample preparation, separation, and purification processes. It also enables the reuse of MMIPs, reducing costs and minimizing waste. These advantages make MMIPs a promising tool in various fields, including environmental monitoring, food analysis, pharmaceutical research, and clinical diagnostics.

Authors' Contributions

RK designed the experiment, wrote, and revised the manuscript. SJD made appropriate changes to finalize the manuscript. All authors approved the final version of manuscript.

Conflict of Interest Disclosures

The authors declare that they have no conflicts of interest.

Acknowledgment

The research work reported here was financially supported by Iran National Science Foundation (INSF).

References

1. Logrieco A, Bottalico A, Mulé G, Moretti A, Perrone G. Epidemiology of toxigenic fungi and their associated mycotoxins for some Mediterranean crops. Epidemiology of Mycotoxin Producing Fungi: Under the aegis of COST Action 835 'Agriculturally Important Toxigenic Fungi 1998–2003', EU project (QLK 1-CT-1998–01380). 2003: 645-67. doi:10.1007/978-94-017-1452-5_1
2. Kabak B, Dobson AD, Var II. Strategies to prevent mycotoxin contamination of food and animal feed: a review. Crit Rev Food Sci 2006;46(8):593-619. doi:10.1080/10408390500436185
3. Zöllner P, Mayer-Helm B. Trace mycotoxin analysis in complex biological and food matrices by liquid chromatography–atmospheric pressure ionisation mass spectrometry. J Chromatogr A. 2006;1136(2):123-69. doi:10.1016/j.chroma.2006.09.055
4. Lattanzio VM, Solfrizzo M, Visconti A. Determination of trichothecenes in cereals and cereal-based products by liquid chromatography–tandem mass spectrometry. Food Addit Contam. 2008;25(3):320-30. doi:10.1080/02652030701513792
5. Gottschalk C, Barthel J, Engelhardt G, Bauer J, Meyer K. Occurrence of type A trichothecenes in conventionally and organically produced oats and oat products. Mol Nutr Food Res. 2007;51(12):1547-53. doi:10.1002/mnfr.200700146
6. Boermans HJ, Leung MC. Mycotoxins and the pet food industry: toxicological evidence and risk assessment. Int J Food Microbiol. 2007;119(1-2):95-102. doi:10.1016/j.ijfoodmicro.2007.07.063
7. Langseth W, Rundberget T. Instrumental methods for determination of nonmacrocyclic trichothecenes in cereals, foodstuffs and cultures. J Chromatogr A. 1998;815(1):103-21. doi:10.1016/S0021-9673(98)00388-4
8. Foroud NA, Eudes F. Trichothecenes in cereal grains. Int J Mol Sci. 2009;10(1):147-73. doi:10.3390/ijms10010147
9. Thrane U, Adler A, Clasen PE, Galvano F, Langseth W, Lew H, et al. Diversity in metabolite production by *Fusarium langsethiae*, *Fusarium poae*, and *Fusarium sporotrichioides*. Int J Food Microbiol. 2004;95(3):257-66. doi:10.1016/j.ijfoodmicro.2003.12.005
10. European Commission, SCOOP TASK 3.2.10. Collection of occurrence data of Fusarium toxins in food and assessment of dietary intake by the population of the EU member states, European Commission, Brussels, Belgium; 2003. Available from: http://ec.europa.eu/food/fs/scoop/task3210.pdf
11. Scudamore KA, Baillie H, Patel S, Edwards SG. Occurrence and fate of *Fusarium mycotoxins* during commercial processing of oats in the UK. Food Addit Contam. 2007;24(12):1374-85. doi:10.1080/02652030701509972
12. Sadok I, Krzyszczak-Turczyn A, Szmagara A, Łopucki R. Honey analysis in terms of nicotine, patulin and other mycotoxins contamination by UHPLC-ESI-MS/MS-method development and validation. Food Res Int. 2023;172:113184. doi:10.1016/j.foodres.2023.113184
13. Trebstein A, Marschik S, Lauber U, Humpf HU. Acetonitrile: the better extractant for the determination of T-2 and HT-2 toxin in cereals using an immunoaffinity-based cleanup?. Eur Food Res Technol. 2009;228:519-29. doi:10.1007/s00217-008-0959-y
14. Biselli S, Hummert C. Development of a multicomponent method for *Fusarium* toxins using LC-MS/MS and its application during a survey for the content of T-2 toxin and deoxynivalenol in various feed and food samples. Food Addit Contam. 2005;22(8):752-60. doi:10.1080/02652030500158617
15. Berthiller F, Schuhmacher R, Buttinger G, Krska R. Rapid simultaneous determination of major type A-and B-

trichothecenes as well as zearalenone in maize by high performance liquid chromatography–tandem mass spectrometry. J Chromatogr A. 2005;1062(2):209-16. doi:10.1016/j.chroma.2004.11.011
16. Schollenberger M, Müller HM, Rüfle M, Suchy S, Plank S, Drochner W. Natural occurrence of 16 *Fusarium* toxins in grains and feedstuffs of plant origin from Germany. Mycopathologia. 2006;161:43-52. doi:10.1007/s11046-005-0199-7
17. De Smet D, Monbaliu S, Dubruel P, Van Peteghem C, Schacht E, De Saeger S. Synthesis and application of a T-2 toxin imprinted polymer. J Chromatogr A. 2010; 1217(17):2879-86. doi:10.1016/j.chroma.2010.02.068
18. Alam MK. Determination of cypermethrin, chlorpyrifos and diazinon residues in tomato and reduction of cypermethrin residues in tomato using rice bran. World. 2013;1(2):30-5. doi:10.12691/wjar-1-2-2
19. Chen D, Deng J, Liang J, Xie J, Huang K, Hu C. Core–shell magnetic nanoparticles with surface-imprinted polymer coating as a new adsorbent for solid phase extraction of metronidazole. Anal Methods. 2013;5(3): 722-8. doi:10.1039/C2AY25897H
20. Chen J, Liang RP, Wang XN, Qiu JD. A norepinephrine coated magnetic molecularly imprinted polymer for simultaneous multiple chiral recognition. J Chromatogr A. 2015;1409:268-76. doi:10.1016/j.chroma.2015.07.052
21. Chen L, Liu J, Zeng Q, Wang H, Yu A, Zhang H, et al. Preparation of magnetic molecularly imprinted polymer for the separation of tetracycline antibiotics from egg and tissue samples. J Chromatogr A. 2009;1216(18):3710-9. doi:10.1016/j.chroma.2009.02.044
22. Chen L, Li B. Determination of imidacloprid in rice by molecularly imprinted-matrix solid-phase dispersion with liquid chromatography tandem mass spectrometry. J Chromatogr B. 2012;897:32-6. doi:10.1016/j.jchromb.2012.04.004
23. Cheong WJ, Yang SH, Ali F. Molecular imprinted polymers for separation science: A review of reviews. J Sep Sci. 2013;36(3):609-28. doi:10.1002/jssc.201200784
24. Davoodi D, Hassanzadeh-Khayyat M, Rezaei MA, Mohajeri SA. Preparation, evaluation and application of diazinon imprinted polymers as the sorbent in molecularly imprinted solid-phase extraction and liquid chromatography analysis in cucumber and aqueous samples. Food Chem. 2014;158:421-8. doi:10.1016/j.foodchem.2014.02.144
25. Ge Y, Butler B, Mirza F, Habib-Ullah S, Fei D. Smart molecularly imprinted polymers: recent developments and applications. Macromol Rapid Commun. 2013; 34(11):903-15. doi:10.1002/marc.201300069
26. Haupt K. Peer reviewed: molecularly imprinted polymers: the next generation. Anal Chem. 2003;75(17):376-A.
27. Haupt K, Mosbach K. Molecularly imprinted polymers and their use in biomimetic sensors. Chem Rev. 2000;100(7):2495-504. doi:10.1021/cr990099w
28. Hernandez F, Sancho JV, Pozo OJ. Critical review of the application of liquid chromatography/mass spectrometry to the determination of pesticide residues in biological samples. Anal Bioanal Chem. 2005;382:934-46. doi:10.1007/s00216-005-3185-5
29. Hu C, Deng J, Zhao Y, Xia L, Huang K, Ju S, et al. A novel core–shell magnetic nano-sorbent with surface molecularly imprinted polymer coating for the selective solid phase extraction of dimetridazole. Food Chem. 2014;158:366-73. doi:10.1016/j.foodchem.2014.02.143
30. Karimian R, Piri F, Hosseini Z. Magnetic molecularly imprinted nanoparticles for the solid-phase extraction of diazinon from aqueous medium, followed its determination by HPLC-UV. J Appl Biotechnol Rep. 2017;4(1):533-9.
31. Ikegami T, Mukawa T, Nariai H, Takeuchi T. Bisphenol A-recognition polymers prepared by covalent molecular imprinting. Anal Chim Acta. 2004;504(1):131-5. doi:10.1016/j.aca.2003.08.032
32. Karimian RA, Piri FA. Synthesis and investigation the catalytic behavior of Cr2O3 nanoparticles. J Nanostruct. 2013;3(1):87-92. doi:10.7508/jns.2013.01.010
33. Li B, Xu J, Hall AJ, Haupt K, Tse Sum Bui B. Water-compatible silica sol–gel molecularly imprinted polymer as a potential delivery system for the controlled release of salicylic acid. J Mol Recognit. 2014;27(9):559-65. doi:10.1002/jmr.2383